 SL, vol.10, no.3, pp.177-199, 2013

Active Control of a Reduced Model of a Smart Structure

N. Ghareeb[1] **and R. Schmidt**[1]

Abstract: Control of vibration plays an important role in the performance of mechanical systems. Moreover, the advances in active materials have made it possible to integrate sensing, actuation and control of unwanted vibration in the design of the structure. In this work, a linear control system based on the Lyapunov stability theorem is used to attenuate the vibration of a cantilevered smart beam excited by its first eigenmode. An optimal finite element (FE) model of the smart beam is created with the help of experimental data. This model is then reduced to a super element (*SE*) model containing a finite number of degrees of freedom (DOF). The damping characteristics are investigated and damping coefficients are calculated and inserted into the model. The controller is applied directly to the SE model and to the extracted state-space (*SS*) representation of the same structure. Finally, results are presented and compared.

Keywords: super element, state-space representation, classical damping, Lyapunov stability theorem

1 Introduction

Weight optimization has a high priority in the design of structures. It has the advantage of reducing the manufacturing and operational costs by reducing the amount of raw material used. Consequently, reducing material results in lower stiffness and less damping which make the structure susceptible to vibration. Beside reducing the performance of the structural system, vibration can also cause fatigue loads that may lead to failure of the structure itself [Ghareeb and Radovcic (2009)].
One of the means to solve this vibration problem is to implement active or smart materials which can be controlled in accordance to the disturbances or oscillations sensed by the structure. Structures incorporating such materials are called smart structures. A smart structure comprises a passive structure and distributed active parts working as sensors and/or actuators. Recent innovations in smart materials coupled with developments in control theory have made it possible to con-

[1] RWTH Aachen University of Technology, Aachen, Germany.

trol the dynamics of structures, and this field is still experiencing large growth in terms of research and development [Vepa (2010)]. Although active vibration control was firstly applied on ships [Mallock (1905)], and after that on aircraft and spacecraft [Vang (1944)], the use of piezoelectric materials as actuators and sensors for noise and vibration control hast been demonstrated extensively over the past thirty years [Piefort (2001)]. Bailey [Bailey (1984)] designed an active vibration damper for a cantilevered beam using a distributed parameter actuator in the form of a piezoelectric polymer. Bailey and Hubbard [Bailey and Hubbard (1985)] developed and implemented three different control algorithms to control the vibration of a cantilevered beam with piezoactuators. Crawley and de Luis [Crawley and de Luis (1987)] and Crawley and Anderson [Crawley and Anderson (1990)] presented a rigorous study on the stress-strain-voltage behaviour of piezoelectric elements bonded to beams, and they observed that in the case of a thin bounding layer, the piezoactuator effective moments can be seen as concentrated on the two ends of the actuator. Fanson and Caughey [Fanson and Caughey (1990)] made use of piezoelectric materials for actuators and sensors and implemented a positive position feedback controller to control the first six bending modes of a cantilevered beam. Hwang and Park [Hwang and Park (1993)] used a constant gain negative velocity feedback controller to attentuate the vibration of a piezolaminated plate. Lim et al. [Lim, Varadan, and Varadan (1997)] used constant gain velocity and constant gain displacement feedback controllers to reduce the vibration amplitude of the first two resonance modes of an aluminium cantilevered piezolaminated plate. Benjeddou [Benjeddou (2000)] presented a survey on the advances in piezoelectric finite element modeling of adaptive structural elements. Manning et al. [Manning, Plummer, and Levesley (2000)] presented a control scheme to control the vibration of a piezoactuated cantilevered beam using system identification and pole placement techniques. Ciaurriz [Ciaurriz (2010)] implemented P and PD controllers to control the vibrations of a flexible piezoelectric beam by using a co-simulation between Adams/Flex and Matlab/Simulink. Kapuria and Yasin [Kapuria and Yasin (2010)] used optimal control strategies with single-input-single-output and multi-input-multi-output configurations to control the vibration in a finite element model of a smart piezolaminated beam including one electric node.

All the works mentioned above emphasize the capabilities and applications of piezoelements as distributed vibration actuators and sensors by simultaneously controling a finite number of modes of the actual system. The majority of the investigations done in this field were carried out either through experiments on an actual model with infinite number of modes, or by using $2D$ or $3D$ FE models of the smart structure. Moreover, the damping coefficients were not calculated but rather assumed, which may not reflect the exact performance of the real model.

The present work comprises the modeling and design of an active linear controller to attenuate the vibration of a cantilevered smart beam excited by its first eigenmode. Firstly, the piezoactuator is modeled, and the relation between voltage and moments at its ends is investigated. A modified FE model of the smart beam based on first-order shear deformation theory ($FOSD$) is then created. The FE model is reduced to a *SE* model with a finite number of DOF, and the damping coefficients are calculated and added to it. The FE and *SE* models are validated by performing a modal analysis and comparing the results with the experimental ones. The *SS* model is extracted too. Finally, the controller which is based on the Lyapunov stability theorem is defined and implemented on the *SE* and the *SS* models of the smart beam. The FE package SAMCEF is used for the creation of the FE and *SE* models, and for the implementation of the controller in the *SE* model. Consequently, Matlab/Simulink is used for the implementation of the controller in the *SS* model.

2 Modeling

In this section, the procedures for modeling a smart structure are examined. The smart structure used in this work is a piezolaminated beam. The same beam model will be used later to extract the *SE* model, derive the *SS* model, and finally, to implement the control strategy. The first step in designing a control system is to build a mathematical model of the structure with all disturbances causing the unwanted vibration. One of the ways to derive the structural analytical model is by using the FE method. The smart beam used consists of a steel beam, a bonding layer and an actuator as seen in **Figure 1**.

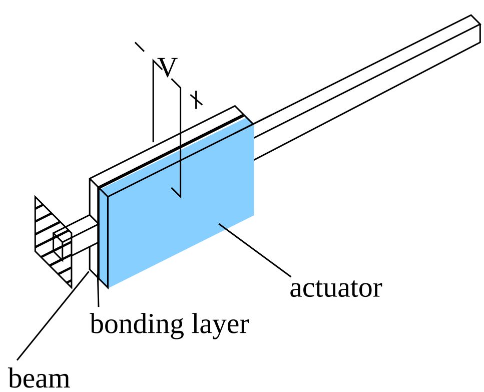

Figure 1: The smart beam

2.1 Actuator modeling

Using an actuator implies implementing an appropriate electric voltage to control the vibration of the smart structure (converse piezoelectric effect). Many FE packages do not offer elements with electrical DOF. Consequently, the voltage applied by the actuator can be represented by two equal moments with opposite directions concentrated at both ends [Crawley and Anderson (1990)]. The relation between actuator moments and actuator voltage can be investigated, so that the moments will then act as the controlling parameters on the smart structure **Figure 2**.

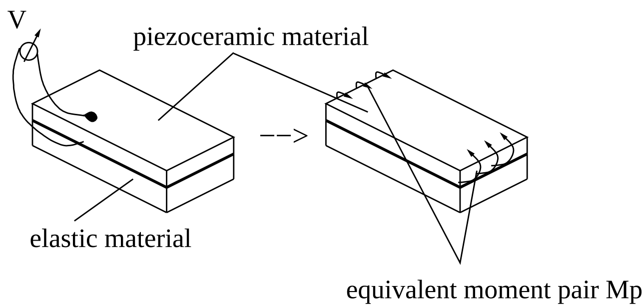

Figure 2: The induced stresses from a piezoceramic actuator

By considering the schematic layout of the middle portion of the smart beam (**Figure 3**), if a voltage V is applied across the piezoelectric actuator, assuming one-dimensional deformation, the piezo-electric strain ε_p of the piezo is:

$$\varepsilon_p = \frac{d_{31}}{t_p} \cdot V \tag{1}$$

where d_{31} is the electric charge constant and t_p is the thickness of the piezoactuator.

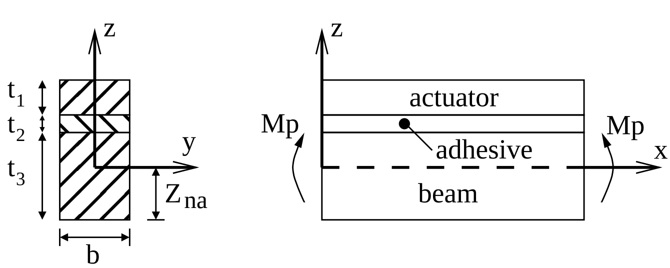

Figure 3: A schematic layout of the composite beam

The longitudinal stress of the piezoactuator can be expressed with Hooke's law as:

$$\sigma_p \;=\; E_p \cdot \varepsilon_p \tag{2}$$

with E_p as its Young's modulus of elasticity.

This stress generates a bending moment M_p (around the neutral axis of the composite beam) given by:

$$M_p \;=\; \int_{(t_a+t_b-Z_{na})}^{(t_p+t_a+t_b-Z_{na})} \sigma_p \cdot b \cdot z\,\mathrm{d}z \tag{3}$$

here, t_a is the thickness of bonding layer (adhesive), t_b is the thickness of beam, b is the width of composite layer at beam's middle, and Z_{na} is the distance from beam's bottom to the neutral axis.

Considering equilibrium of moments (about the neutral axis) yields:

$$\int_{beam} \sigma_b\,\mathrm{d}A \;+\; \int_{adhesive} \sigma_a\,\mathrm{d}A \;+\; \int_{piezo} \sigma_p\,\mathrm{d}A \;=\; 0 \tag{4}$$

After integrating (4), the position of the neutral axis Z_{na} can be found:

$$Z_{na} \;=\; \frac{E_p t_p^2 + 2E_p t_p t_a + 2E_p t_p t_b + E_a t_a^2 + 2E_a t_a t_b + E_b t_b^2}{2E_p t_p + 2E_a t_a + 2E_b t_b} \tag{5}$$

where t_p is the thickness of the piezo, E_a is Young's modulus of adhesive and E_b is Young's modulus of the beam.

Combining (1),(2),(3) and (5) together determines the actuator bending moment M_p as a function of the voltage V:

$$M_p = \frac{E_p E_a (t_p t_a + t_a^2) + E_p E_b (t_b^2 + t_p t_b + 2t_a t_b)}{E_p t_p + E_a t_a + E_b t_b} \cdot \frac{d_{31} \cdot b}{2} \cdot V \tag{6}$$

Since the relation between M_p and V is now known, the actuator moment is taken instead of the voltage as input to the controller that will be later designed and implemented. From now on, there will be only mechanical *DOF* in the model.

2.2 *FE* modeling

The resultant FE model of the smart beam must be faithfully representative in order to use it for further applications like control analysis. To find the best FE model, the optimal element type and size must be selected. Thus, a modal analysis of the real beam is experimentally performed and results of the natural frequencies are compared with those from the FE model where different element types are used. A detailed geometry of the smart beam is shown in **Figure 4**, and the material properties and thickness of each part are represented in **Table 1**.

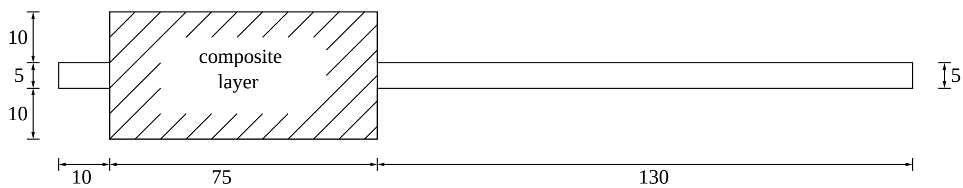

Figure 4: A detailed geometry of the smart beam [dimensions in *mm*]

Table 1: Parameters of the components of the smart beam

	Beam	Bonding	Actuator
Material	steel	epoxy resin	$PIC151$
Thickness [mm]	0.5	0.036	0.25
Density [kg/m^3]	7900	1180	7800
Young's mod. [MPa]	210000	3546	66667

The smart beam is created as a unique structure but modeled as a composite shell with three layers. This means, all the three components of the model, i.e. beam, bonding layer and actuator are bonded together without any relative slip among the contact surfaces. Consequently, each layer has its own mechanical properties. To validate the choice of the FE type used (a composite shell element with 8 nodes based on the $FOSD$), a modal analysis of the FE model is done and the first two eigenfrequencies are read and compared to those from the experiment. This is seen in **Table 2**. As a boundary condition, the far left edge of the smart beam is clamped.

Concerning the optimal FE size to be used, it's well known that reducing the FE size will improve the solution accuracy. However, especially in the case of large

Table 2: Validation of element-type based on the modal analysis

	FE model	Experiment
$1st$ eigenfrequency $[Hz]$	13.81	13.26
$2nd$ eigenfrequency $[Hz]$	42.67	41.14

complex structures, the use of excessively fine elements in the FE model may result in unmanageable computations that exceed the memory capabilities of existing computers [Ko and Olona (1987)]. From **Table 3**, it is seen that using an element

Table 3: Effect of element size on the eigenfrequency

FE size $[mm]$	$1st$ eigenfreq. $[Hz]$	$2nd$ eigenfreq. $[Hz]$
0.25	13.80	42.66
0.5	13.81	42.66
1.0	13.81	42.67
2.5	13.83	42.71
5	13.89	42.81
10	14.09	43.21

size less than 1 *mm* does not make any significant change on the values of the $1st$ and $2nd$ eigenfrequencies of the smart beam. This means, it can be regarded as the optimal value for the element size in the FE modeling.

Before this subsection is closed, it may be argued that the damped frequency from experimental modal analysis of the real model was compared to the undamped frequency of the FE model, where the damping coefficients are not yet calculated. This is true, but it does not have a big influence on the solution since the relation between the damped and the undamped frequencies in terms of the damping ratio ξ is

$$\omega_{damped} = \omega_{undamped} \sqrt{1-\xi^2} \tag{7}$$

Thus, a direct comparison between both frequencies can be made since $\xi \ll 1$.

2.3 SE modeling

A super element, also termed substructure, is a complex element that includes a number of finite elements used in a structural modeling. The main virtue of this technique is the ability to perform the analysis of a complete structure by using the results of prior analysis of different regions comprising the whole structure [Ghareeb and Weichert (2009)]. The application of the *SE* technique goes back to the early 1960s when it has been used by aerospace engineers to break down the structure of an airplane into simpler first-level substructures for enhancing the computaional efficiency [Fan, Tang, and Chow (2004)].
The basic concept of substructuring is that all DOF, which are considered useless for the final solution, are condensed and the rest is retained. This means, the *DOF* of the whole system correspond to the retained nodes plus a number of internal deformation modes (dynamic analysis problems).
To construct a *SE*, or in other words to remove the unwanted nodes and *DOF* from the substructure, the method of "component mode synthesis" is used [Craig and Bampton (1968)], and a linear *SE* is created. According to this method, the *DOF* of each substructure are classified into:

1. Boundary DOF shared by several structures
2. Internal DOF belonging only to the considered substructure

The behaviour of each substructure is described by the combination of two types of component modes:

1. The constraint modes (static deformed shape) which are determined by assigning a unit displacement to each boundary DOF, while all other boundaries DOF are being fixed
2. The normal vibration modes (dynamic deformed shape) that correspond to the vibration modes obtained by clamping the structure at its boundary

It is then assumed that the behaviour of the substructure in the global system can be represented by superimposing the constrained modes and a small number of normal vibration modes. Taking an infinite number of modes would not help and does not make sense since only a few number of modes has a physical meaning [Hughes (1987)]. Hence, by retaining only the low-frequency vibration modes, the substructure's dynamically deformed shape can be represented with sufficient accuracy.

Starting from the FE model of the previous subsection, a *SE* model with a limited number of DOF will be created.

Firstly, the master or retained nodes must be selected. These correspond to the nodes where a boundary condition or a load is applied. The rest of the nodes will be considered as slave or condensed nodes. In the FE model, 5 nodes are considered as retained nodes **(Figure 5)**.

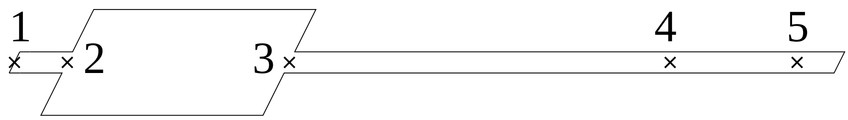

Figure 5: The retained nodes of the *SE*

This means:

- *Node* 1 is used to introduce a boundary condition (clamping constraint).
- *Node* 2 is used to introduce a load (actuator moment).
- *Node* 3 is used to introduce a load (actuator moment).
- *Node* 4 is used to measure the displacement (distance sensor).
- *Node* 5 is used to measure the tip displacement (distance sensor).

Secondly, 10 modes, which correspond to 97% of the modal effective mass, are selected. The percentage of modal effective mass for each mode is usually found inside the input file created by any FE software.
To check the validity of the *SE* created, it has to be compared to the FE model which was already validated before. Abstractly said, the reduced model must have the same characteristics as the original model, except that the number of nodes is reduced, as well as the number of DOF. The eigenfrequencies of the first 2 modes resulting from each model are depicted in **Table 4**.

Table 4: Eigenfrequencies of the first two modes

Mode	*SE* model [Hz]	FE model [Hz]	Experiment [Hz]
1	14.249	13.811	13.26
2	43.414	42.673	41.14

The physical properties of each model are shown in **Table 5**. It is clear that both models deliver almost the same value of the eigenfrequency for the first two modes. Since the excitation of the beam by its first eigenmode is concerned, furhter readings are not necessary. Compared to the FE model, the SE model has few number of DOF and a very small number of nodes. It consists of a single element and has the advantage that the simulation time becomes short and the controllers are implemented on the SE model itself.

Table 5: Characteristics of the FE and SE models

	FE model	SE model
Element size [mm]	3.07	
Number of elements	2575	1
Number of nodes	8206	5
Number of DOF	16860	40

3 Damping Characteristics

Damping of structures has historically been of great importance in nearly all branches of engineering endeavors. Mechanical and structural systems rely on various damping mechanisms to dissipate energy during undesirable vibratory motions [Taylor and Nayfeh (1997)]. Damping parameters, which are also of significant importance in determining the dynamic response of structures, cannot be deduced deterministically from other structural properties or even predicted by using the FE technique. For this reason, recourse must be made to data from experiments conducted on completed structures of similar characteristics. Such data is scarce in general, but they are very valuable for studying the phenomenon and modeling of damping [Butterworth, Lee, and Davidson (2004)]. In fact, there are many non-linear damping models available [Puthanpurayil, Dhakal, and Carr (2011)], but in this work the damping is assumed to be viscous and frequency dependent for the sake of convenience and simplicity [Alipour and Zareian (2008)].
With this linear approach, which was initially introduced by Rayleigh [Rayleigh (1877)], it is supposed that the damping matrix is in a linear combination of the mass and stiffness matrices. Although this idea was suggested for mathematical convenience only, it allows the damping matrix to be diagonalized simultaneously with the mass and stiffness matrices, preserving the simplicity of uncoupled, real normal modes as in the undamped case [Adhikari and Woodhouse (2001)]. The

relation is:

$$C = \alpha M + \beta K \tag{8}$$

where α and β are real scalars that must be determined.

The main advantage of this formulation is that the damping matrix will be a diagonal matrix. The damping ratio ξ is related to the scalars α and β through the relation [Ghareeb and Schmidt (2012)]:

$$\xi_i = \frac{\alpha}{2\,\omega_i} + \beta\,\frac{\omega_i}{2} \tag{9}$$

with ω as the eigenfrequency and the subscript i the mode number.

Here, two values for the eigenfrequency ω_i with the corresponding values of ξ_i are needed to find out the scalars α and β and thus to compute the damping matrix C. Two methods are used to find these damping characteristics. These are the method of Chowdhury and Dasgupta [Chowdhury and Dasgupta (2003)], and the method of damping from normalised spectra, also known as the half-power bandwidth method [Butterworth, Lee, and Davidson (2004)],[Ewins (1984)]. Results from both methods are represented in **Table 6**.

Table 6: Results of α and β from both methods

	Chowdhury	Half-power bandwidth
α	0.02577	0.02955
β	9.918×10^{-6}	9.770×10^{-6}

It can be noticed that both methods have shown that the damping is mass proportional, since $\alpha \gg \beta$ in both techniques. In this work, the average values of both methods are used, and the damping characteristics are added to the *SE* model and to the *SS* representation that will be derived in the next section.

4 State-Space Representation

4.1 Basics of the state-space representation

Beside the *SE* model, the *SS* representation is used as a second approach to implement the controller. The basic idea of this procedure is to describe a system of

equations in terms of n first-order differential equations. Hence, the use of vector-matrix notation greatly simplifies the mathematical representation of the system of equations. On the other hand, the increase in the number of state variables, the number of inputs, or the number of outputs does not increase the complexity of these equations [Ogata (2002)]. This approach is used here in order to validate or compare the results of the *SE* model.
The state equations have the form:

$$\begin{aligned} \dot{x} &= A\,x + B\,u \\ y &= C\,x \end{aligned} \tag{10}$$

and the size of the matrices A, B and C depends on the number of states, inputs and outputs of the system. Upon specifying the type and position of the input and output vectors, a FORTRAN code is used to create the *SS* model of the smart beam. This model is then integrated in Matlab/SIMULINK to give the dynamic response of the modelled structure under one or several inputs and outputs.

4.2 Creation and validation of the SS equations for the case of a smart beam

The objective now is to create the *SS* representation of the smart structure investigated in this work, and to validate it by carrying out a simple simulation, so that the results can be compared to those from the *FE* model. At the beginning, the inputs and outputs of the system must be specified. Referring to **Figure 5**, a sensor is placed at *Node* 5 to measure the tip displacement, and the input will be a harmonic force at the same node. Thus, the smart beam will be excited by its first eigenmode. The force F has the form:

$$F = c\,\sin(\omega_1\,t); \qquad \text{with } c \text{ as a constant (amplitude)} \tag{11}$$

Now, there is a single input and a single output. Since *Node* 1 is clamped, the number of states is defined as:

$$2p = 30 + 10 - 6 = 34 \tag{12}$$

There are 30 *DOF* in the system, in addition to 10 vibration modes. Concerning the dimensions of the matrices A, B, C:

$$\begin{aligned} dim(A) &= 34 \times 34 \\ dim(B) &= 34 \times 1 \\ dim(C) &= 1 \times 34 \end{aligned} \tag{13}$$

The *SS* representation of this smart beam is shown in **Figure 6**. The simulation is carried out for 40 seconds while the load is kept active for the first 20 seconds. The resulting curve in **Figure 7** shows that both models had the same value of tip displacement throughout the simulation time. This gives more reliance to the results. However, both models will be used in the coming section for the implementation of the controller.

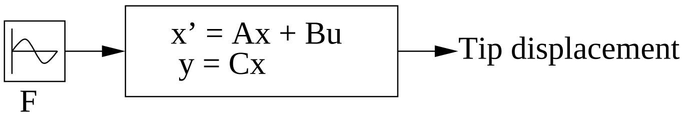

Figure 6: The *SS* model of the smart beam

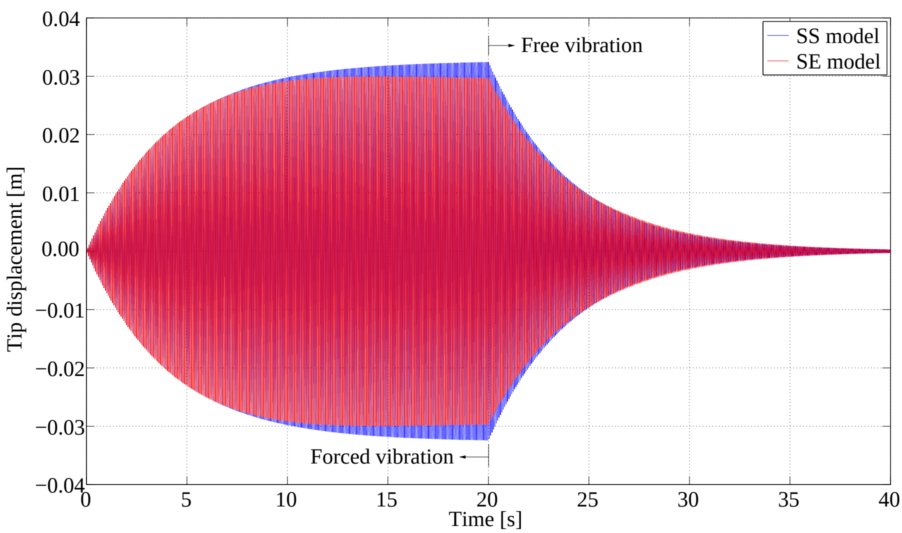

Figure 7: Free and forced vibration of the smart beam

5 Controller Design

5.1 Lyapunov Stability Theorem Controller

Although there is no general procedure for constructing a Lyapunov function, yet any function can be considered as a candidate if it meets some requirements, i.e., positive definite, equal to zero at the equilibrium state and with its derivative less or equal to zero [Khalil (1996)],[Bacciotti and Rosier (2005)]. Now, the energy equation of a thin Bernoulli-Euler beam which is modelled as a single FE in a one-dimensional system with length h and left point coordinate x_i, is considered as a Lyapunov function candidate **(Figure 8)**.

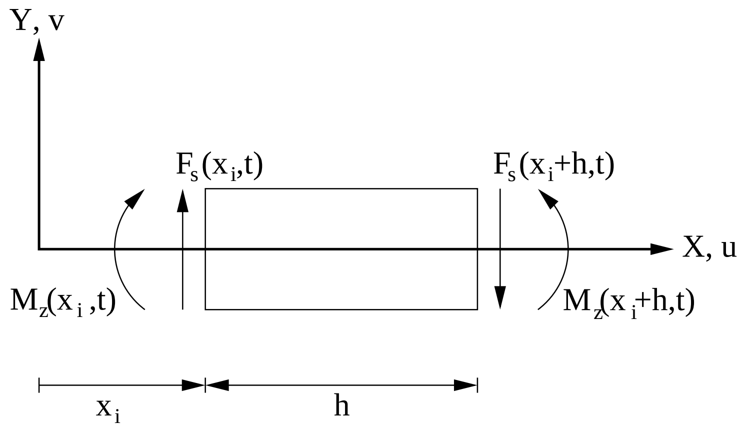

Figure 8: Section of the smart beam where the piezoelement is located

According to [Gorain and Bose (1999)], the total energy equation of a beam without any external forces or moments is:

$$U = \frac{1}{2}\int_{x_i}^{x_{i+h}} \left[\rho A\left(\frac{\partial v}{\partial t}\right)^2 + EI\left(\frac{\partial^2 v}{\partial x^2}\right)^2\right] \mathrm{d}x \tag{14}$$

where h is the length of the beam section, u and v are the displacements in longitudinal and transverse directions, E and ρ are the elastic modulus and density of the beam.
According to **Figure 8**, M_z is the actuator bending moment, F_s is the shear force on the beam, and I_z is the second moment of inertia of its cross-section about the (bending) z-axis.

The above function is locally positive definite, continuously differentiable and equal to zero at the equilibrium state. Yet, to consider it as a Lyapunov function, the derivative of this function must be smaller or less than zero as well.
Differentiating (14) in time leads to:

$$\dot{U} = \int_{x_i}^{x_{i+h}} \left[\rho A\frac{\partial v}{\partial t}\frac{\partial^2 v}{\partial t^2} + EI\frac{\partial^2 v}{\partial x^2}\frac{\partial}{\partial t}\left(\frac{\partial^2 v}{\partial x^2}\right)\right] \mathrm{d}x \tag{15}$$

Referring to the relationships for a vibrating beam, which are summarized in any reference about beams like [Petyt (2003)], it reveals that:

$$\begin{aligned}
\rho A\frac{\partial^2 v}{\partial t^2} + EI\frac{\partial^4 v}{\partial x^4} &= 0 \\
M_z &= EI\frac{\partial^2 v}{\partial x^2} \\
F_s &= -EI\frac{\partial^3 v}{\partial x^3}
\end{aligned} \tag{16}$$

Substituting the derived equations for the bending moment M_z, shear force F_s, and assuming no shear after that, the first derivative yields:

$$\dot{U} = M_z\left[\frac{\partial}{\partial t}\left(\frac{\partial v}{\partial x}\right)\right]_{x_i}^{x_i+h} = M_z\left(\dot{v}\prime_{x_i+h} - \dot{v}\prime_{x_i}\right) \tag{17}$$

where $\dot{v}\prime_{x_i}$ is a rotational velocity at node x_i.
To ensure that (17) is always smaller or equal to zero, M_z, the actuator moment, can have the value:

$$M_z = -k\left(\dot{v}\prime_{x_i+h} - \dot{v}\prime_{x_i}\right) \tag{18}$$

with k as a positive constant, sometimes called "the proportionality factor". Varying k has a significant effect on the response. Theoretically, the system is stable for any positive value. Nevertheless, larger values of k tend to "overcontrol the structure" since the moment will have a magnitude larger than that required. Consequently, if k is very small, the added moments will be insufficient and this will reduce the damping ratio. Therefore, a trial-and-error procedure is required to select the best value and customize the control to the application [Newman (1992)].

Substituting (18) in (17) yields:

$$\dot{U} = -k\left(\dot{v}\prime_{x_i+h} - \dot{v}\prime_{x_i}\right)^2 \leq 0 \tag{19}$$

and thus, all the requirements to have a Lyapunov function are met. Therefore, (18) can be used as the controller for the smart beam.
To implement this equation on the smart beam, the moments at *node* 2 and *node* 3, which are equal in magnitude but with opposite directions, are calculated as functions of the rotational velocites at both nodes [Ghareeb and Schmidt (2012)]. They have the form:

$$\begin{aligned}
M_{2y} &= -k\left(\dot{v}_{2y} - \dot{v}_{3y}\right) \\
M_{3y} &= -k\left(\dot{v}_{3y} - \dot{v}_{2y}\right)
\end{aligned} \tag{20}$$

From the above equations, it is clear that the controller is in fact a connection between the *DOF* of the nodes composing the *SE*. To do that in SAMCEF, the nonlinear forces element (FNLI) is used. This element allows the introduction of a list of n general linear or nonlinear internal forces as a function of list of n *DOF* and their derivatives. The control strategy is defined directly inside the input file without the use of any external programming language, and this is one of the merits of the *SE* technique.

Coming back to the control law of (20), the controller is stable for any positive value of the constant k. At the beginning, three different values of k are taken, and the results are depicted in **Figure 9**.

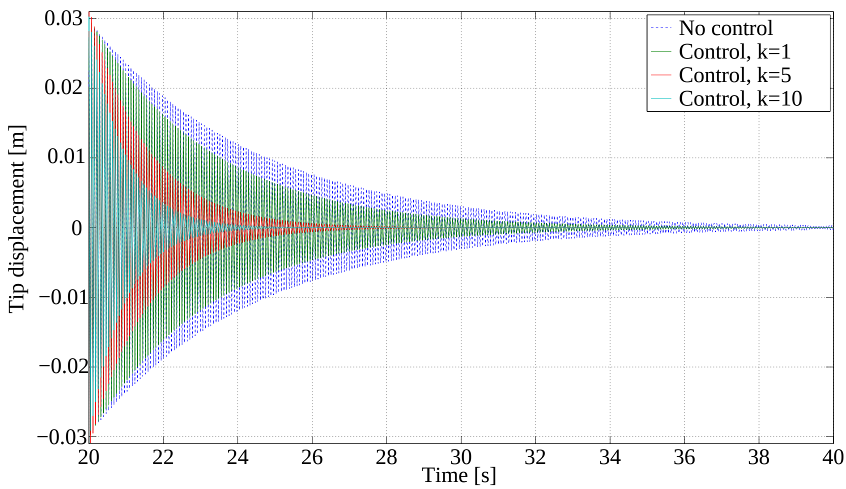

Figure 9: The Lyapunov stability theorem controller for different values of k (*SE* model)

Moreover, the choice of k has an influence on the amplitude of the resonance at the natural frequency of the structure, which is seen in **Figure 10**. Now, the optimal value of the constant k must be found. Since the design of optimal controllers is not the task of this work, the method of trial-and-error is used to find out this optimal value. Best results are got for $k = 30$, and the corresponding curve of tip displacement vs. time of the smart beam is illustrated in **Figure 11**. In the FFT spectrum diagram **(Figure 12)**, the effect of the controller on the amplitude of the resonance at the natural frequency is shown as well.

As stated before, the *SS* representation of the smart beam is derived in order to validate the results from the *SE* model. To do that, the inputs and the outputs are

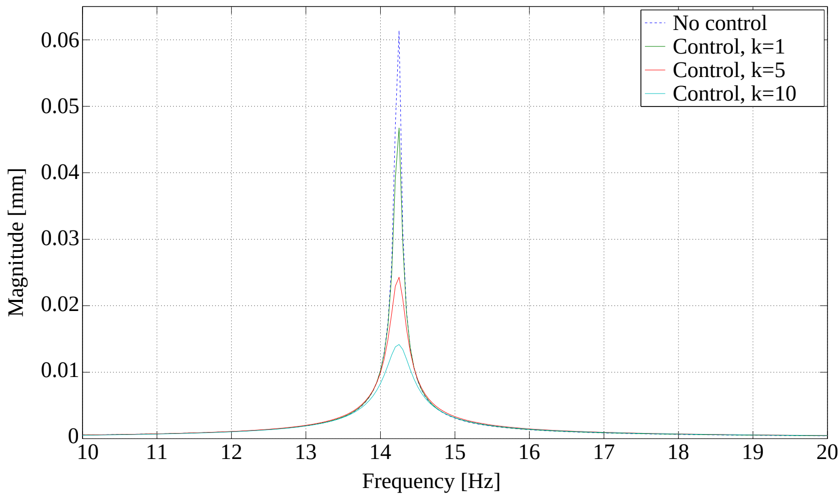

Figure 10: The FFT spectrum of the smart beam for different values of k (*SE* model)

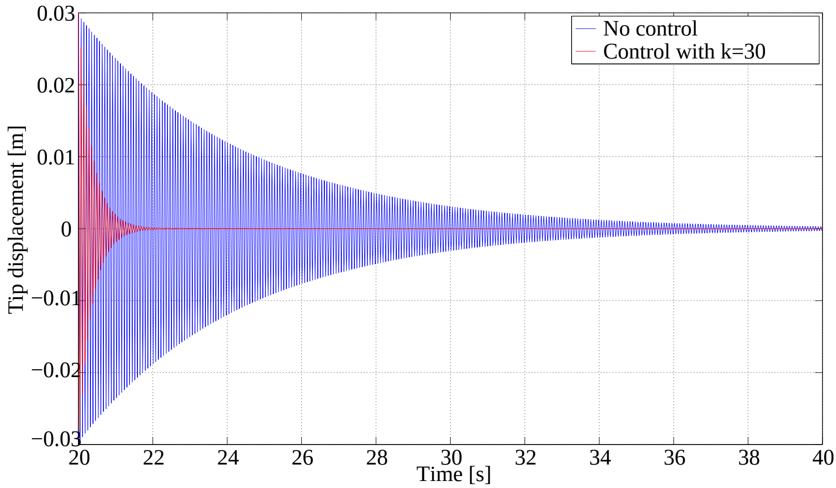

Figure 11: The Lyapunov stability theorem controller for $k = 30$ (*SE* model)

designated in order to find out the matrices A, B and C of (10). To implement the controller in the *SS* model, two steps are performed. In step one, the only input to the system is the forced excitation until the magnitude of vibration does not change anymore, i.e., up to $t = 20s$, and the output consists of the tip displacement, as

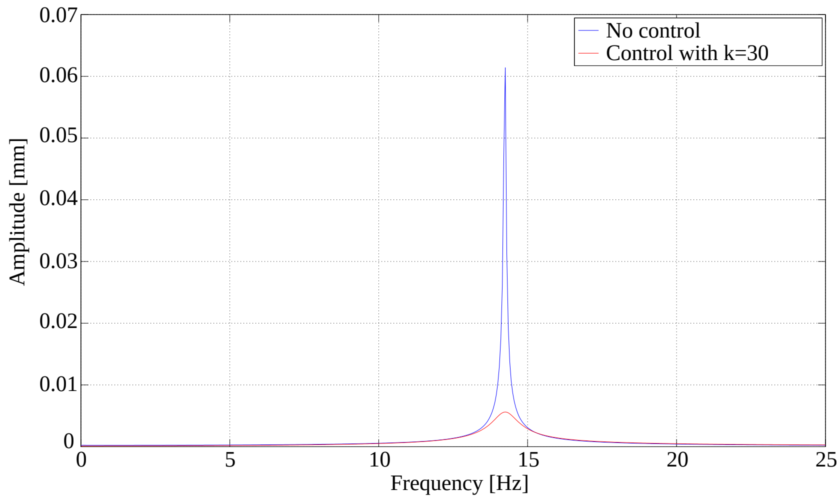

Figure 12: The FFT spectrum of the smart beam using Lyapunov stability controller (*SE* model)

well as the state vectors exactly at $t = 20s$. The diagram is shown in **Figure 13**.

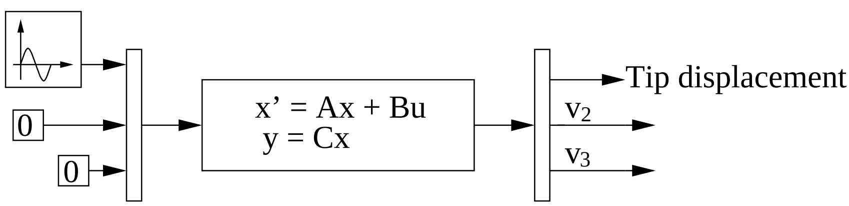

Figure 13: The *SS* model of the smart beam with controller (step 1)

These state vectors are then fed in as initial conditions in the second step. This time, the input comprises both actuator moments at both ends of the actuator, and the output embraces the tip displacement at *node* 5, and the velocities at the *node* 2 and *node* 3.
The steps mentioned above could be also summarized in one step, but in this case a timer must be inserted in the model to deactivate the exciting force when vibrations become stable at $t = 20s$. The *SS* representation of the smart beam in the second step is shown in **Figure 14**.
A comparison of the results from the *SE* model and the *SS* model is shown in

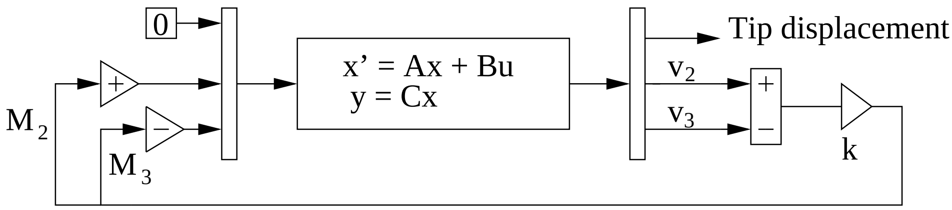

Figure 14: The *SS* model of the smart beam with controller (step 2)

Figure 15 and **Figure 16** where the time region between 20 and 22 *s* is magnified. It can be seen that both models yielded the same results. Nevertheless, much more

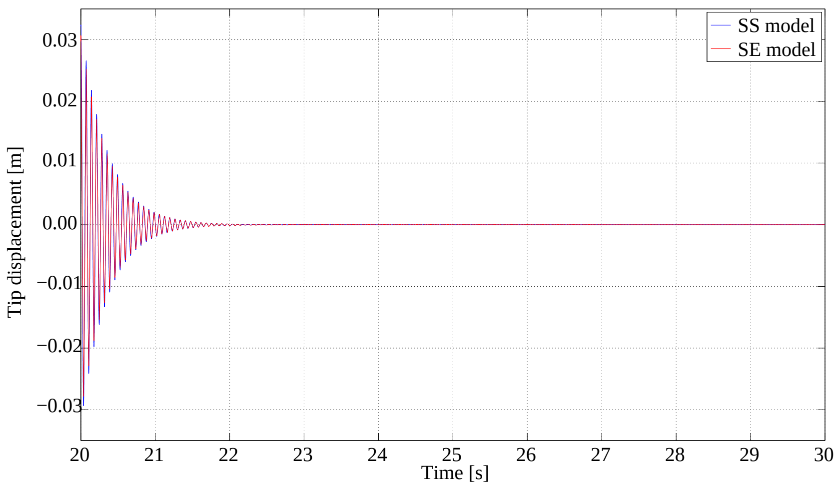

Figure 15: Tip displacement vs. time using *SE* and *SS* models

time was needed to carry out the simulation in the *SS* model (about 35 minutes), while in the *SE* model, less time (only 3 minutes) was needed. This could be due to the fact that in the *SE* model a fixed time-step can be assigned (here 0.01 *s*), while in the *SS* representation the time-step was automatically set. Moreover, the stresses and energy curves, could be requested in addition to the force vectors along the *SE* model. This is one of the advantages of the *SE* technique in comparison to the *SS* representation which is more practical and in which the controller can be easily implemented [Ghareeb and Schmidt (2012)].

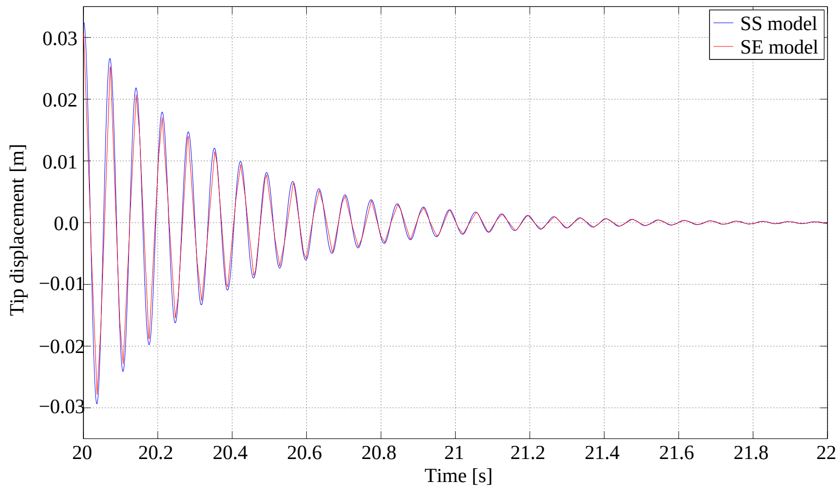

Figure 16: Tip displacement vs. time in a zoomed region of Figure 15

6 Summary

In this work, a linear controller based on the Lyapunov stability theorem was designed and implemented on a reduced model of a smart structure. The super element technique was used to create this reduced model starting from the finite element model. A state-space representation of the same model was extracted as well. The controller was implemented on this model too, and the results from both models were compared.

References

Adhikari, S.; Woodhouse, J. (2001): Identification of damping: Part 1, viscous damping. *Journal of Sound and Vibration*, vol. 243, pp. 43–61.

Alipour, A.; Zareian, F. (2008): Study rayleigh damping in structures; uncertainties and treatments. In *the 14th world conference on earthquake engineering*.

Bacciotti, A.; Rosier, L. (2005): *Liapunov Functions and Stability in Control Theory*. Springer.

Bailey, T. (1984): Distributed-parameter vibration control of a cantilever beam using a distributed-parameter actuator. Master's thesis, Massachusetts Institute of

Technology (MIT), 1984.

Bailey, T.; Hubbard, J. J. (1985): Distributed piezoelectric-polymer active vibration control of a cantilever beam. *AIAA Journal of Guidance and Control*, vol. 6, No. 5, pp. 605–611.

Benjeddou, A. (2000): Advances in a piezoelectric finite element modeling of adaptive structural elements: a survey. *Computers and Structures*, vol. 76, pp. 347–363.

Butterworth, J.; Lee, J.; Davidson, B. (2004): Experimental determination of modal damping from full scale testing. In *13th world conference on earthquake engineering*.

Chowdhury, I.; Dasgupta, S. (2003): Computation of rayleigh damping coefficients for large systems. *The electronic Journal of geotechnical engineering*, vol. 8.

Ciaurriz, P. (2010): Active vibration control of a flexible beam by using a co-simulation of adams/flex and matlab/simulink. Master's thesis, RWTH Aachen University of Technology, 2010.

Craig, R. R.; Bampton, M. (1968): Coupling of substructures for dynamic analyses. *AIAA Journal*, vol. 6, pp. 1313–1319.

Crawley, E.; Anderson, E. (1990): Detailed models of piezoelectric actuation of beams. *Journal of Intelligent Material Systems and Structures*, vol. 1, pp. 4–24.

Crawley, E. F.; de Luis, J. (1987): Use of piezoelectric actuators as elements of intelligent structures. *AIAA Journal*, vol. 25, No. 10, pp. 1373–1385.

Ewins, D. J. (1984): *Modal Testing*. John Wiley & Sons Inc.

Fan, J. P.; Tang, C. Y.; Chow, C. L. (2004): A multilevel superelement technique for damage analysis. *International Journal of Damage Mechanics*, vol. 13, pp. 187–199.

Fanson, J.; Caughey, T. (1990): Positive position feedback control for large space structures. *AIAA Journal*, vol. 28, pp. 717–724.

Ghareeb, N.; Radovcic, Y. (2009): Fatigue analysis of wind turbines. *DEWI magasin*, vol. 35, pp. 12–16.

Ghareeb, N.; Schmidt, R. (2012): Modeling and active vibration control of a smart structure. *Proceedings of the 9th international Conference on Informatics in Control, Automation and Robotics (ICINCO 2012), Rome, Italy*, vol. 1, No. 86, pp. 142–147.

Ghareeb, N.; Weichert, D. (2009): Combined multi-body-system and finite element analysis of a complex mechanism. *Proceedings of the 11th SAMCEF User Conference, Paris.*

Gorain, G. C.; Bose, S. K. (1999): Boundary stabilization of a hybrid euler-bernoulli beam. In *Proc. Indian Acad. Sci. (Math. Sci.).*

Hughes, P. C. (1987): Space structures vibration modes: How many exist? which ones are important? *IEEE Control Systems Magazine*, pp. 22–28.

Hwang, W.; Park, H. (1993): Finite element modeling of piezoelectric sensors and actuators. *AIAA Journal*, vol. 31, No. 5, pp. 930–937.

Kapuria, S.; Yasin, M. (2010): Active vibration control of piezoelectric laminated beams with electroded actuators and sensors using an efficient finite element involving an electric node. *Smart Mater. Struct.*, vol. 19, pp. 1–15.

Khalil, H. (1996): *Nonlinear Systems*. Prentice Hall, Madison.

Ko, W.; Olona, T. (1987): Effect of element size on the solution accuracies of finite-element heat transfer and thermal stress analysis of space shuttle orbiter. Memorandum 88292, NASA, 1987.

Lim, Y.; Varadan, V.; Varadan, V. (1997): Closed loop finite element modeling of active structural damping in the frequency domain. *Smart Mater. Struct.*, vol. 6, pp. 161–168.

Mallock, A. (1905): A method of preventing vibration in certain classes of steamships. *Trans. Inst. Naval Architects*, vol. 47, pp. 227–230.

Manning, W.; Plummer, A.; Levesley, M. (2000): Vibration control of a flexible beam with integrated actuators and sensors. *Smart Mater. Struct.*, vol. 9, pp. 932–939.

Newman, S. M. (1992): Active damping control of a flexible space structure using piezoelectric sensors and actuators. Master's thesis, Naval Postgraduate School, 1992.

Ogata, K. (2002): *Modern Control Engineering*. Prentice Hall.

Petyt, M. (2003): *Introduction to Finite Element Vibration Analysis*. Cambridge University Press.

Piefort, V. (2001): *Finite Element Modelling of Piezoelectric Active Structures*. PhD thesis, Université Libre de Bruxelles, Belgium, 2001.

Puthanpurayil, A.; Dhakal, R.; Carr, A. (2011): Modelling of in-structure damping: A review of the state-of-the-art. In *Proceedings of the ninth pacific conference on earthquake engineering, Auckland, New Zealand.*

Rayleigh, L. (1877): *Theory of Sound*. Dover Publications.

Taylor, T. W.; Nayfeh, A. H. (1997): Damping characteristics of laminated thick plates. *Journal of Applied Mechanics*, vol. 64, pp. 132–138.

Vang, A. (1944): Vibration dampening, 1944. Patent No. 2,361,071, USA.

Vepa, R. (2010): *Dynamics of Smart Structures*. John Wiley & Sons Ltd.